Research in Astronomy and Astrophysics, 23:055010 (9pp), 2023 May https://doi.org/10.1088/1674-4527/acc14e


# Investigation on the Formation of Herringbone Structure in Type II Solar Radio Bursts

Z. Z. Abidin, A. N. Zulkiplee, V. Epin, and F. A. M. Pauzi
Radio Cosmology Research Lab, Physics Dept., Faculty of Science, University of Malaya, Kuala Lumpur, Malaysia; zzaa@um.edu.my
*Received 2022 November 23; revised 2023 January 25; accepted 2023 February 2; published 2023 April 26*

## Abstract

We report detailed observation of the "herringbone" of a Type II solar radio burst that occurred on 2010 November 3rd. Data from the Space Weather Prediction Center, National Oceanic and Atmospheric Administration, e-CALLISTO, and Nançay RadioHeliograph are analyzed. We determine the brightness temperature and degree of circular polarization of the "herringbone" burst. Correlations between the physical parameters and the "herringbone" are examined. Based on the relationship, this is the first study that suggested this "herringbone" was generated through fundamental plasma.

*Key words:* Sun: activity – Sun: corona – Sun: coronal mass ejections (CMEs) – Sun: magnetic fields – Sun: radio radiation

## 1. Introduction

An emission of radio energy from the Sun into the interplanetary medium is commonly acknowledged as a solar radio burst (Pauzi et al. 2020). The common types of radio bursts are distinguishable with low frequency from as low as below 200 MHz. However, consideration involving other frequency ranges should be taken into account as some of the latest publications reported to have bursts identified to be outside of the previously reported range. According to Wijesekera et al. (2018), the first phenomenon identified in the field of radio astronomy was solar radio bursts. Solar radio bursts have been classified into five main types: I, II, III, IV, and V where each type has their own frequency range commonly detected. Type II solar radio bursts will be the main subject of this research.

The formation of Type II bursts is said to be caused by magnetohydrodynamic shock waves that accompany the coronal mass ejections (CMEs) (Zucca et al. 2012). Based on Monstein (2012), Type II bursts are narrow bands of strong radiation that drift slowly, and at times irregularly, toward lower frequencies after large flares. White (2007) stated: "Type II bursts typically occur at around the time of the soft X-ray peak in a solar flare." Type II bursts are easily distinguishable from Type III bursts because the frequency drift is typically two orders of magnitude slower than that of the fast drift Type III bursts; hence the name slow drift burst.

Occasionally, Type II bursts can be seen to exhibit fundamental and harmonic emission in frequency albeit the complexity makes it difficult to identify them. A unique feature called "herringbones" among Type II bursts has also been detected in rare occurrence (Monstein 2012). Based on this structure, the velocity of the solar disturbance that produces these slow drift bursts can be deduced from the rate of frequency change. The velocity should be on the order of 1000 $\mathrm{km\,s^{-1}}$ which is associated with superalfvén shocks which appear in solar flares and CMEs that propagate through the solar corona (Monstein 2012).

The emission mechanism of Type II bursts may have originated from the plasma emission at the plasma frequency and its harmonic. Generally, a Type II burst is a low frequency phenomenon that can be detected below 100 MHz. Plasma radiation or so-called plasma frequency makes up Type II solar radio bursts. This radiation is related to a collisionless shock whereas the emission processes require the conversion of Langmuir waves into electromagnetic radiation (Melrose 1980; Cairns & Robinson 1987). According to Roberts (1959), in about 20% of Type II bursts, short duration bursts are found superimposed on the Type II radiation. Generally, these bursts appear in groups on both the fundamental and second harmonic bands of Type II. These bursts have narrow bandwidths and very rapid frequency drift rates. An individual burst may occur as if originates near the center of either the fundamental or harmonic band of the Type II case and can drift to either higher or lower frequencies with time. Roberts (1959) first observed the phenomenon of "herringbone" emission and considered it as groups of fast-drift bursts seeming to emanate from the drifting bands of Type II solar radio bursts.

CALLISTO stands for Compact Astronomical Low-cost Low-frequency Instrument for Spectroscopy and Transportable Spectrometers. It is a type of radio spectrometer with world-wide usage for 24/7 surveillance of solar activities (Antar et al. 2014; Abidin et al. 2015; Pauzi et al. 2020). Currently, there is a network of more than 144 instruments constructed at more

**Table 1**
Solar Radio Burst Type Details from NOAA

| Flare Begin Time | Flare Peak Time | Flare End Time | Flare Class | Particular | Frequency (MHz) |
|---|---|---|---|---|---|
| 12:07 UT | 12:21 UT | 12:33 UT | C4.9 | Type II (herringbone) | 150–450 |

than 80 locations globally for studying the meter and decameter bands. The management of CALLISTO occurs through an international collaboration with the Swiss Federal Institute of Technology Zürich (ETHZ). CALLISTO is capable of detecting frequencies spanning 45 to 870 MHz (Antar et al. 2014).

In this paper, a detailed and comprehensive observational physical description of "herringbone" bursts is presented with regard to how this burst is formed or generated. It is important to study this burst because it is one of the unique features of Type II solar radio bursts. A Type II solar radio burst is quite special compared to other types of bursts as it has features such as fundamental and harmonic emissions and of course the "herringbones" (Monstein 2012; Pauzi et al. 2020). However, many researchers mainly focus on the fundamental and harmonic emission and less on "herringbone" structure because the latter is a rare occurrence compared to the former. The methodology for the observations is discussed in Section 2. In Section 3, the results are presented, and discussion based on the results is explained. In Section 4, we discuss the concluding summary on the "herringbones" of Type II solar radio bursts based on the relationship with the physical parameters associated with their formation.

## 2. Observation

Data from the Space Weather Prediction Center, National Oceanic and Atmospheric Administration (SWPC, NOAA) showed that a C4.9 class flare and a Type II solar radio burst occurred on 2010 November 3rd. Table 1 reports the details of the solar radio burst Type II taken from the NOAA archive data during the event. This Type II solar burst detection with unique "herringbones" structure was also confirmed by Zimovets et al. (2012).

Data from e-CALLISTO showed a Type II solar radio burst with the unique feature of "herringbones" appearing at 12:15:00 UT on 2010 November 3rd. Data used throughout these observations were taken from Bleien Observatory (BLEN7M) and from HUMAIN Observatory with period from 12:15:00 UT to 12:20:00 UT and plotted together as shown in Figure 1. Type II solar radio bursts are commonly detected in the range of frequency from 200 to 500 MHz. Before the formation of Type II solar radio bursts, a C4.9 class flare occurred from 12:07:00 UT to 12:33:00 UT and the flare peaked at 12:21:00 UT. The purplish-black horizontal line

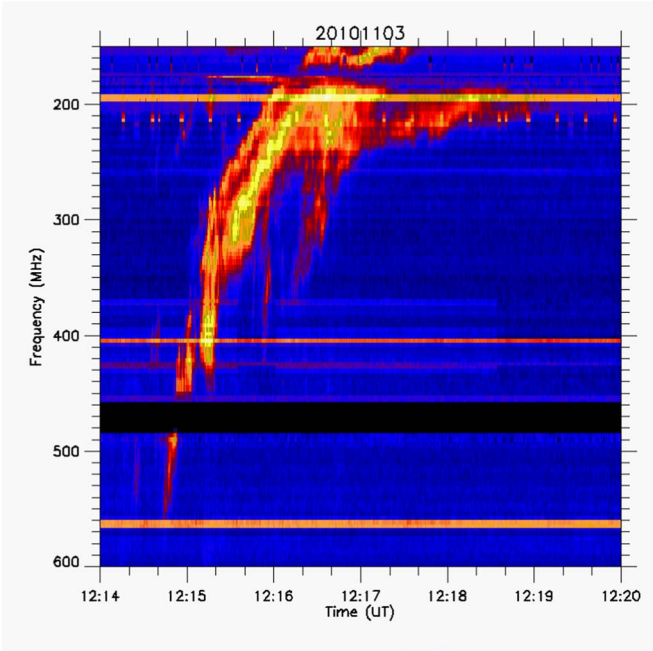


**Figure 1.** Dynamic spectrum of a Type II solar radio burst showing a "herringbones" feature on 2010 November 3rd. This is a combined spectrum from BLEN7M (180–600 MHz) and HUMAIN (150–180 MHz). "Herringbones" start at 12:15:00 UT and last until 12:18:00 UT.

across the spectrum is radio frequency interferences (RFIs). CALLISTO can be seriously affected by RFI in the radio frequency below 870 MHz where the ranges can vary. For instance, the first range is between 80 and 110 MHz while the second range is between 460 and 500 MHz. Although at 270–290 MHz, CALLISTO stations around the world are free of RFI, the radio telescopes are often uncalibrated due to uncertainties from antenna gain as a result of a wide frequency range. Not only that, antenna patterns, low region ionospheric solar signal dispersion, and of course RFI are also not calibrated. Consequently, the data obtained are severely affected. Ground-based solar radio observation activities, especially employing CALLISTO instruments, have the greatest exposure to this RFI hazard (Abidin et al. 2015). Man-made radio signals with different times and frequencies are very powerful throughout the radio spectrum because they are easily

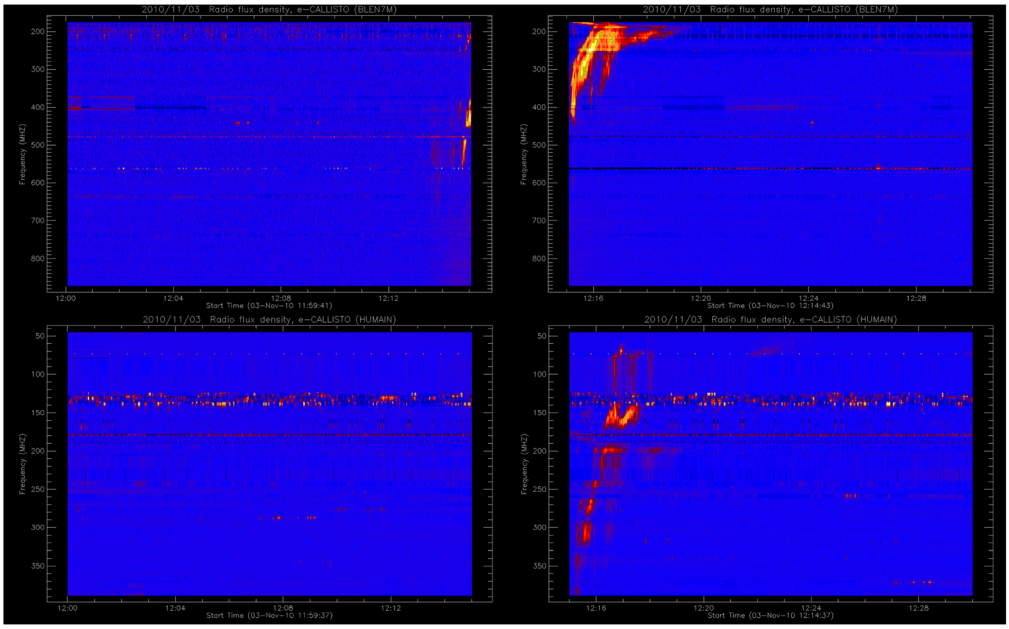


**Figure 2.** The spectra from BLEN7M (200–800 MHz) and HUMAIN (50–350 MHz).

recognizable in the lobe far outside CALLISTO from the primary beam of the antenna (Abidin et al. 2015).

We retrieved four data files from the e-CALLISTO website, two from BLEN7M and two from HUMAIN as displayed in Figure 2. Among the four data, three of them show visible frequency drift in the spectral images of the Type II solar radio bursts while the other one does not show obvious frequency drift. The one that does not show frequency drift also has some interference in the spectral image. For clarity and to have a general understanding of the source region, we resorted to use data from the Nançay RadioHeliograph (NRH). NRH can provide a variety of data types including an animation of the data, brightness temperature, and data on degree of polarization up to ten frequencies within 150–445 MHz. The time cadence is 5 ms, and the spatial resolution is 0.′3–6′, depending on the observing frequency. We only used 1 s of integrated data (Liu et al. 2018).

We carefully examined the images of several wavelengths and multi-frequency results of the NRH radio sources from 12:15:15 UT to 12:17:15 UT in Figure 3 with a 40 ms interval between the first and next image. A contour of 95% of the maximum intensity is drawn for NRH sources. From the animation of the data, the radio sources can be seen to remain stationary throughout the surge of the Type II solar radio burst. The radio sources of all ten NRH frequencies line up very well, stretching from the lower flaring site to the higher corona.

In the field of radio astronomy, brightness temperature ($T_B$) is widely used as a measure of received intensity. The definition of brightness temperature can be derived from Plank's blackbody radiation law (Alley & Jentoft-Nilsen 1999)

$$T_B \equiv \frac{c^2 I_f}{2f^2 k_B} = \frac{\lambda^2 I_\lambda}{2k_B}, \quad (1)$$

($T_B$ is the brightness temperature; $c$ is the speed of light; $I_f$ is the intensity of the radiation at frequency $f$; $f$ is the frequency of the radiation; $k_B$ is the Boltzmann constant; $\lambda$ is the wavelength of the radiation; $I_\lambda$ is the intensity of the radiation at wavelength $\lambda$). Hence, the formal definition of brightness temperature is the temperature at which a blackbody in thermal equilibrium with its surroundings would have to be in order to duplicate the observed intensity of an object at a frequency $f$ (Alley & Jentoft-Nilsen 1999).

An important property of electromagnetic wave propagation is the polarization of the electric field ($E$), which is defined by the orientation of the $E$ vector as it varies in time. At each point during a polarization state, the electromagnetic field of the wave has a constant magnitude and is rotating at a constant rate in a plane perpendicular to the direction of the wave. In a circularly polarized wave, the electromagnetic wave can rotate in two possible directions such as right-handed (clockwise) and left-handed (counter-clockwise) (Toh et al. 2003). The degree of circular polarization ($q$) is defined by the Stokes $V$ component over the Stokes $I$ component as follows in Equation (2) (Liu et al. 2018)

$$q = \frac{V}{I}. \quad (2)$$

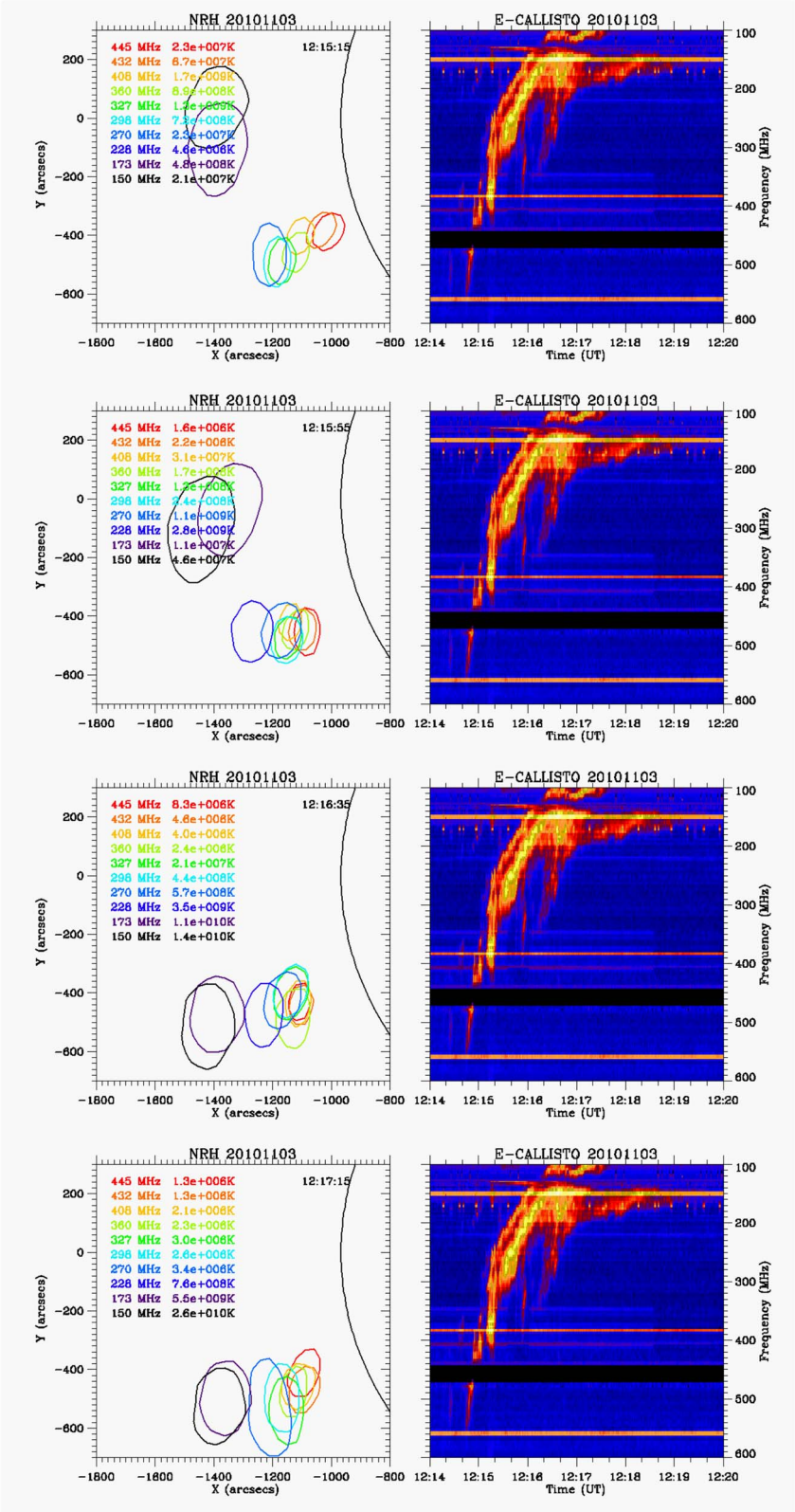


**Figure 3.** Overplotted spectrum with NRH radio frequencies at 10 frequencies during the "herringbones". The contours are 95% of the maximum value. From 12:15:15 UT to 12:17:15 UT, the radio source of each frequency remains stationary. These images also work as animation.

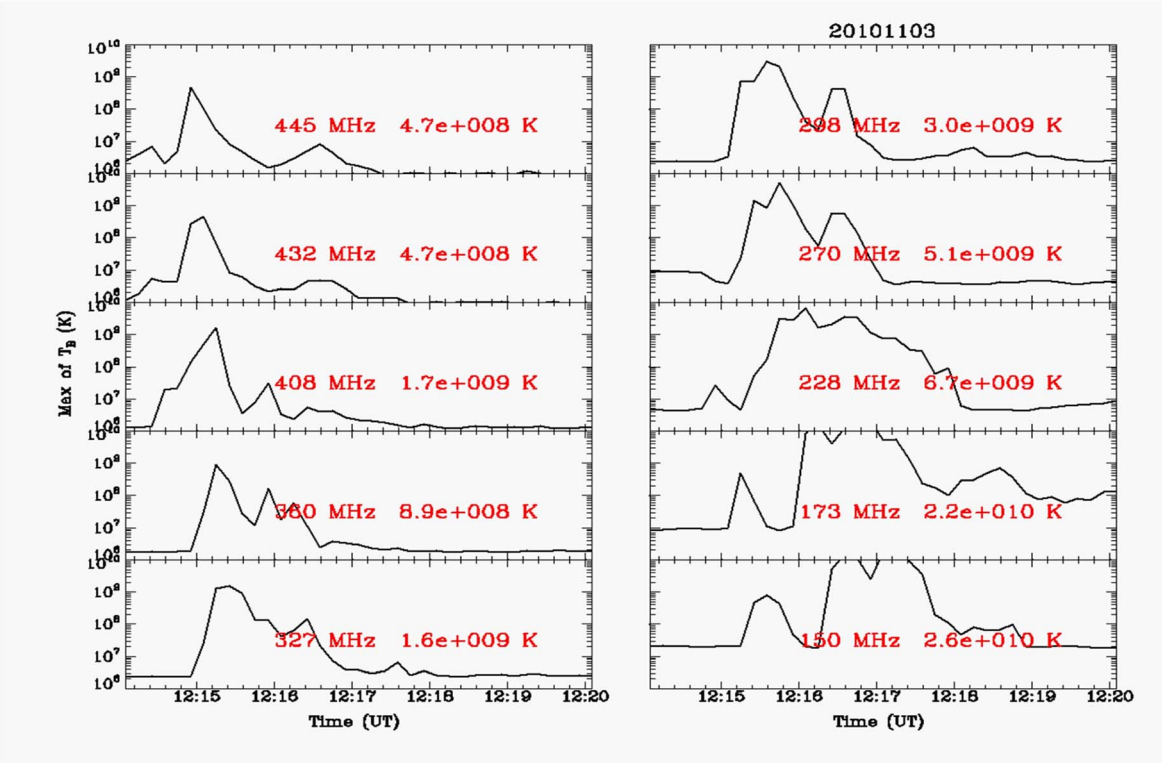


**Figure 4.** Brightness temperatures of NRH frequencies from 12:15:00 UT to 12:20:00 UT on 2010 November 3rd. The rising in values of brightness temperatures signifies the beginning of the "herringbone" whereas the drop in values means ending of the "herringbone."

## 3. Results and Discussion

The maximum brightness temperatures, $T_B$ values, observed at NRH frequencies and their time dependencies are plotted (Figure 4). An average $T_B$ of all pixels within the 95% maximum contour is presented. The maximum $T_B$ values at all frequencies are above $10^8$ K. The maximum $T_B$ at 150 MHz even exceeds $10^{10}$ K for several minutes. It was found that the decrease in frequency will result in better $T_B$ and vice versa (Liu et al. 2018). From around 12:15:00 UT, $T_B$ values at all frequencies started to rise to higher values. Apart from this, at around 12:18:00 UT, $T_B$ values at lower frequencies started to drop to lower values. A rise of the frequencies for $T_B$ values at 12:15:00 UT marked the beginning of the "herringbones" of the Type II solar radio burst whereas the drop of the low frequency (228 MHz, 150 MHz) $T_B$ values at 12:18:00 UT signified the decrease of frequency spectrum and ending of the "herringbones" of the Type II solar radio burst.

The time dependence of the degree of circular polarization is plotted (Figure 5). The average $q$ of all pixels within the 95% maximum contour is used. Throughout the "herringbones" of a Type II solar radio burst, $|q|$ remains steady at values from as low as 4% to as high as 52% (4%–52%). At the same time, most of the $q$ values (445 MHz, 432 MHz, 408 MHz, 270 MHz, 228 MHz, 173 MHz, 150 MHz) are negative, which indicates left-handed circular polarization (Vasanth et al. 2016; Liu et al. 2018; Vasanth et al. 2019).

There are four main different types of radiation mechanisms that can be utilized to interpret this "herringbones" Type II solar radio burst (Table 2). To determine the appropriate mechanism, we consider the main observational characteristics of this event of a solar radio burst. The observational characteristics of different types of solar radio bursts and their underlying radiation mechanisms have been summarized by Dulk (1985). We focus on the radiation mechanisms in this case; the important physical parameters such as brightness temperature and degree of circular polarization are emphasized.

The physical parameters of the 2010 November 3rd event are listed in the bottom row of the table. First, an important characteristic is the extremely high brightness temperature ($\sim 10^{10}$ K). This indicates that it must be either the fundamental plasma or 2nd harmonic plasma or electron-cyclotron maser (ECM) emission. Second, the polarization degree is around 4%–52%, which precludes that this originated from the 2nd harmonic plasma or ECM emission.

By taking high $T_B$ and the polarization degree, the only feasible mechanism is the fundamental plasma. This is consistent with earlier theoretical study by Cairns & Robinson (1987).

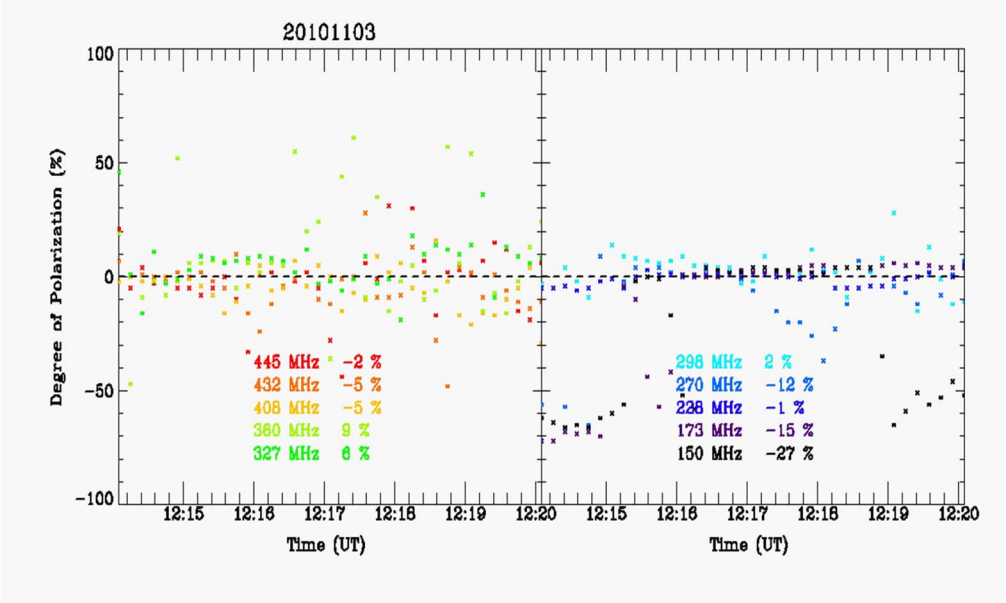


**Figure 5.** Degree of Polarization ($q$) of NRH frequencies from 12:15:15 UT to 12:18:05 UT.

**Table 2**
Characteristics of Various Radiation Mechanisms (Liu et al. 2018) and Our Observation

| Mechanism | $T_B$ | Polarization ($\|q\|$) | Reference |
|---|---|---|---|
| Cyclotron | $<10^9$ K | Any | (Dulk 1985) |
| Synchrotron | $<10^9$ K | 0% (Linear) | (Dulk 1985) |
| Gyrosynchrotron | $<10^9$ K | Any | (Robinson 1978a) |
| Fundamental Plasma | $\geqslant 10^9$ K | ∼100%–0% | (Robinson 1978b) |
| 2nd harmonic plasma | $\leqslant 10^{13}$ K | <10% | (Melrose 1975) |
| ECM emission | $\geqslant 10^{10}$ K | ∼100% | (Winglee 1985) |
| Type II herringbone on 2010-11-03 | $10^{10}$ K | 4%–52% | ⋯ |

**Note.** $T_B$ refers to the brightness temperature and $q$ means the degree of circular polarization. The observational parameters of Type II "herringbones" on 2010 November 3rd are also listed for comparison.

Based on research conducted by Cairns & Robinson (1987) as well as Cane & White (1989), the "herringbone" bursts are plasma radiation generated by electron streams accelerated at the Type II shock. Electron streams which are accelerated by the Type II shock caused "herringbone" bursts as radiation at multiples of the plasma frequency. According to another study by Roberts (1959): "Herringbones bursts are plasma radiation resulting from Langmuir waves generated by energetic electron streams accelerated at the Type II shock." Generally, "herringbone" bursts move from higher frequencies to lower frequencies. This then corresponds to electron streams moving away from the Sun and is also known as forward bursts (Cairns & Robinson 1987). This statement agrees with our spectrum image of "herringbone" as plotted earlier (refer to Figure 1).

The radiation mechanisms of the "herringbones" bursts might not necessarily be fundamental plasma but can be 2nd harmonic plasma as well since this type of radiation mechanism is also a type of plasma radiation. Cairns & Robinson (1987) summarized the maximum brightness temperature of the "herringbone" bursts according to their radiation mechanism (fundamental plasma or 2nd harmonic plasma) as follows

$$1 \times 10^{10}\,\mathrm{K} < T_B(f) < 6 \times 10^{11}\,\mathrm{K},$$

and

$$2 \times 10^{8}\,\mathrm{K} < T_B(h) < 2 \times 10^{11}\,\mathrm{K},$$

where $T_B(f)$ is the maximum brightness temperature for fundamental plasma and $T_B(h)$ is for 2nd harmonic plasma. We can see that the two maximum brightness temperatures show obvious differences in which $T_B(f)$ is at extremely high brightness temperature while $T_B(h)$ is at slightly lower brightness temperature than that of $T_B(f)$. Based on our data, the maximum brightness temperature of the "herringbone" of the Type II solar radio burst on 2010 November 3rd is $4.7 \times 10^8$ K $< T_B < 2.6 \times 10^{10}$ K. At first glance, this event seems to be following the radiation mechanism of the 2nd harmonic plasma. However, this is not enough to justify the type of radiation mechanism. We need additional information on the physical parameters (Cairns & Robinson 1987).

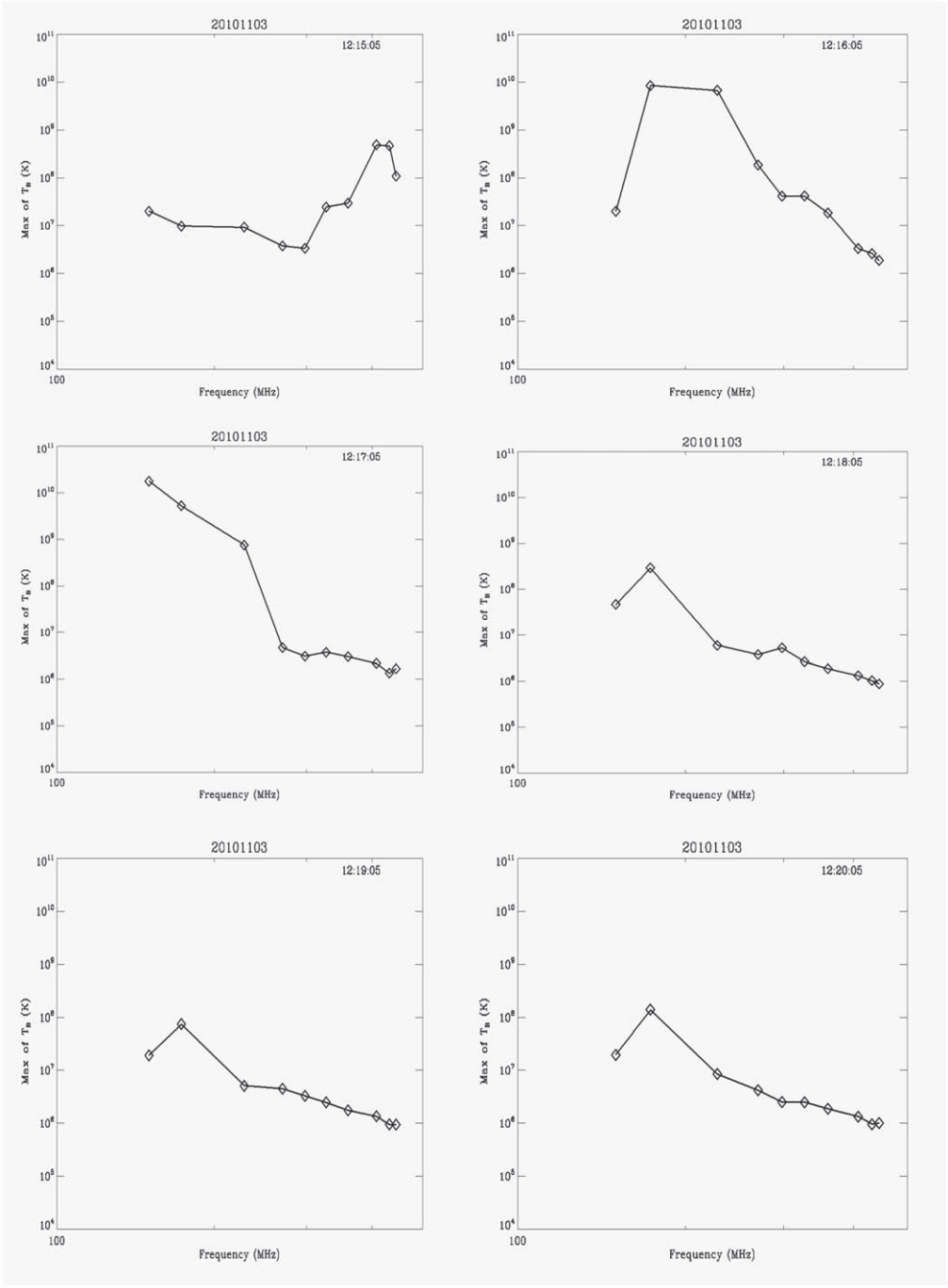


**Figure 6.** Linear fit of the maximum brightness temperature from 12:15:05 UT to 12:20:05 UT on 2010 November 3rd. The dots are the brightness temperature data of ten NRH frequencies (150–445 MHz).

Polarization degree can provide the information that we require. According to a study by Stewart (1966), the circular polarization of "herringbone" bursts ranged from less than 10% to more than 70%. This also coincides with the polarization degree of our event (4%–52%). Then, it becomes more obvious that the radiation mechanism of our "herringbone" follows the fundamental plasma.

"Herringbone" bursts generally occur in tight groups composed of a few to as many as 100 individual bursts (Cairns & Robinson 1987). Based on the linear fit of the maximum

brightness temperature (Figure 6), the values of the brightness temperature reached their peak of $10^{10}$ K at 12:16:05 UT and began to decrease at 12:17:05 UT. Comparing this to the spectrum image of the event (Figure 1), we can see that at these times, the bursts are at the frequency between 200 and 250 MHz which means the burst is broad and concentrated. This may indicate that individual "herringbones" are distributed throughout the group.

The structure of "herringbones" strongly depends upon the intensity of its Type II bursts. According to Cane & White (1989), about 21% of all Type II bursts show herringbone structure, and about 60% of the most intense bursts contain a "herringbone." Based on the conclusions derived from the study by Cairns & Robinson (1987), they concluded several different deductions, one of them is that "herringbones" tend to occur in "clumps" or groups, rather than occurring uniformly throughout the Type II event. This is the same as the "herringbone" in our observation. We can see that from 12:16:05 UT until 12:17:05 UT, most of the bursts are concentrated and distributed at frequency between 200 and 250 MHz while some bursts or "clumps" of bursts are distributed unevenly at frequency above 250 MHz around the same time. This shows that our observation agrees with the conclusion deduced by Cairns & Robinson (1987).

## 4. Conclusions

This work highlights the importance of finding the "herringbone" structures in other event observations for future studies. A Type II solar radio burst with a "herringbone" on 2010 November 3rd was studied in this work. We can see that the radio sources of various NRH frequencies remain stationary instead of propagating. We also notice that the NRH sources at different frequencies line up very well. The physical parameters of the "herringbone" were also studied. The brightness temperatures of different frequencies were extremely high. They all exceeded $10^8$ K with the maximum brightness temperature at $10^{10}$ K even for 150 MHz. In general, lower frequency had higher $T_B$. The degree of circular polarization was between $4\% \sim 52\%$ and was highly left-hand circularly polarized (Vasanth et al. 2016; Liu et al. 2018; Vasanth et al. 2019).

The possible radiation mechanisms based on the physical parameters were also summarized. From the high $T_B$ and high $|q|$, we conclude that this "herringbone" of a Type II solar radio burst is generated through fundamental plasma. According to Cane & White (1989), "The production of "herringbones" is either by facilitating the production of Type-II like streams of electrons or if energetic electrons are continuously produced, the local conditions could control their access to field lines on which they can travel the distances implied by the frequency drifts."

We conducted this study using the data from SWPC, NOAA, e-CALLISTO, and imaging data at metric wavelengths from the NRH. NRH provides observations between 150 and 445 MHz. Imaging data from NRH can provide information on the physical parameters such as spatial dispersion of radio sources, brightness temperature, and degree of polarization (Vasanth et al. 2016; Liu et al. 2018; Vasanth et al. 2019). From these, we can know that the unique "herringbone" feature of a Type II solar radio burst has stationary radio sources, extremely high brightness temperature ($10^8$ K–$10^{10}$ K), and high polarization degree (4%–52%). Based on the relationship between these physical parameters and a "herringbone" burst, we can see that a "herringbone" is generated from a Type II solar radio burst that follows fundamental plasma.

As we have mentioned before, "herringbones" are fundamentally "clumps" or groups of individual Type II bursts that are distributed throughout the spectrum (Cairns & Robinson 1987; Cane & White 1989). Not all Type II solar radio bursts have these "herringbones." Only those with intense Type II bursts have this feature, which is the condition for the generation of "herringbones" to appear most favorable when the Type II solar radio bursts follow fundamental plasma. This is because the emission mechanism based on fundamental plasma has higher maximum brightness temperature and degree of circular polarization when compared to 2nd harmonic plasma. Higher maximum brightness temperature and degree of circular polarization correspond to intense Type II solar radio bursts.

## Acknowledgments

The authors would like to acknowledge the Faculty of Science, University of Malaya (grant No. GPF081-2020) for their funding. The authors would also like to thank the Institute for Data Science FHNW Brugg/Windisch, Switzerland for availability of e-CALLISTO data.

*Data Availability:* The data sets generated during and/or analyzed during the current study are available from the corresponding author on reasonable request.

*Declaration of Competing Interest:* The authors declare that they have no known competing financial interests or personal relationships that could have appeared to influence the work reported in this paper.

## ORCID iDs

A. N. Zulkiplee https://orcid.org/0000-0003-1410-6052

## References

Alley, R., & Jentoft-Nilsen, M. 1999
Abidin, Z. Z., Anim, N. M., Hamidi, Z. S., et al. 2015, NewAR, 67, 18
Antar, Y., Zawari, A., Islam, M. T., et al. 2014, IAPM, 56, 278
Cairns, I., & Robinson, R. 1987, SoPh, 111, 365
Cane, H., & White, S. 1989, SoPh, 120, 137
Dulk, G. A. 1985, ARA&A, 23, 169
Liu, H., Chen, Y., Cho, K., et al. 2018, SoPh, 293, 1

Melrose, D. 1980, The Emission Mechanisms for Solar Radio Bursts (New York: Gordon and Breach)
Melrose, D. 1975, SoPh, 43, 211
Monstein, C. 2012, RadA, 7, 63
Pauzi, F., Abidin, Z. Z., Guo, S. J., et al. 2020, SoPh, 295, 1
Roberts, J. 1959, AuJPh, 12, 327
Robinson, R. 1978a, ApJ, 222, 696
Robinson, R. 1978b, SoPh, 60, 383
Stewart, R. 1966, AuJPh, 19, 209
Toh, B. Y., Cahill, R., & Fusco, V. F. 2003, ITEdu, 46, 313
Vasanth, V., Chen, Y., Feng, S., et al. 2016, ApJL, 830, L2
Vasanth, V., Chen, Y., Lv, M., et al. 2019, ApJ, 870, 30
White, S. M. 2007, AsJPh, 16, 189
Wijesekera, J., Jayaratne, K., & Adassuriya, J. 2018, JPhCS, 1005, 012046
Winglee, R. M. 1985, Radio Stars (Berlin: Springer), 49
Zimovets, I., Vilmer, N., Chian, A.-L., Sharykin, I., & Struminsky, A. 2012, A&A, 547, A6
Zucca, P., Carley, E., McCauley, J., et al. 2012, SoPh, 280, 591